12 Mar 1991, 2:30 pm - 3:30 pm

Estimation of Amplification Spectra for P and SV Waves

Ken'ichi Abe
Kumagai Gumi Co., Ltd., Tokyo, Japan

Kin'ichi Kasuda
Kumagai Gumi Co., Ltd., Tokyo, Japan

Michiyasu Terada
Kumagai Gumi Co., Ltd., Tokyo, Japan

Teruo Shimizu
Kumagai Gumi Co., Ltd., Tokyo, Japan

Proceedings: Second International Conference on Recent Advances in Geotechnical Earthquake Engineering and Soil Dynamics, March 11-15, 1991, St. Louis, Missouri, Paper No. 8.19

:stimation of Amplification Spectra for P and SV Waves

en'ichi Abe
umagai Gumi Co., Ltd., Tokyo, Japan

Kin'ichi Kasuda
Kumagai Gumi Co., Ltd., Tokyo, Japan

lichiyasu Terada
umagai Gumi Co., Ltd., Tokyo, Japan

Teruo Shimizu
Kumagai Gumi Co., Ltd., Tokyo, Japan

YNOPSIS: In order to evaluate site effects on strong ground motions,the earthquake motions btained from the vertical array deploying toward the depth of 400m and a part of the atellite array around its array are used. Dividing horizontal and vertical time histories nto two potions which have primary and secondary arrivals respectively,their amplification pectral ratios between particular two points in and around the vertical array are examined s a problem of incident P- and SV-wave into stratified structures.

INTRODUCTION

In earthquake engineering, it has been recently recognized as one of the most important problems to evaluate site effects on strong ground motion. A great variety of topographic and geologic conditions of a site would affect its strong ground motion, and that would make it difficult to evaluate site effects. Since our engineering structures have been constructed on these sites, to clarify site effects on strong ground motion is also a great problem on the practical dynamic design. In spite of such difficulty, site effects on strong ground motions have been actually estimated as the amplification factors in the case of the SH-wave incidence to the stratified soils. On the other hand, with recent advancement of earthquake proof design, dynamic design is being required not only in horizontal direction but also in vertical direction. Thereby, with regard to the evaluation of site effects, vertical motions can not be neglected as well as the problem of horizontal motions. As far as the authors are aware, there have been little discussion on evaluating site effects in vertical direction.

In this paper, using recorded motions of the vertical array deployed toward the depth of 400m under the ground, amplification factors of vertical motions are examined in comparison with horizontal motions. Assuming that vertical motions are composed of body waves, amplification factors would be given as the transfer ratio on P and SV-wave incidence. Here, both recorded motions in vertical and horizontal direction are divided into two portions (; Primary and Secondary portion assumed to be composed of P and SV-wave respectively), and their amplification spectral ratios between particular two points in the vertical array are compared with the theoretical ratios in the case of P-and SV-wave incidence to the stratified soils. In addition, comparing outcrop motions on rock sites to underground motions in their identical layers, site effects on outcrop motions are evaluated,and it is examined whether our rock sites can be regarded as a standardized point to estimate amplification factors.

CHARACTERISTICS OF THE ARRAY OBSERVATION SYSTEM AND RECORDED MOTIONS

The dense instrument array observation system "KASSEM" has been developed, and more than hundred earthquakes have been observed on the coastal area in Miyagi and Fukusima prefecture since 1984.9. As shown in Figure 1, KASSEM consists of Center Array (C.A.) and Strong Motion Array (S.M.A.) systems. C.A. is three-dimensionally deployed with 14 seismographs (three components type) on and under the ground. In addition, S.M.A. consists of 8 seismographs on the ground and covers wide areas. This array forms the " simple extended array" with C.A. which is classified into the "local laboratory array". The system contents will not be described more over since there exists reference (1) which dealt with in detail.

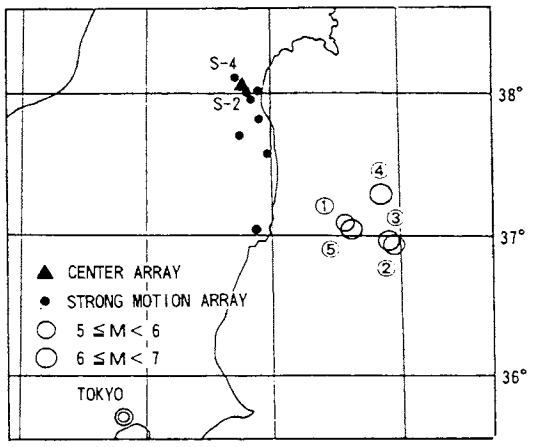

Figure 1 The locations of observation site and epicenters

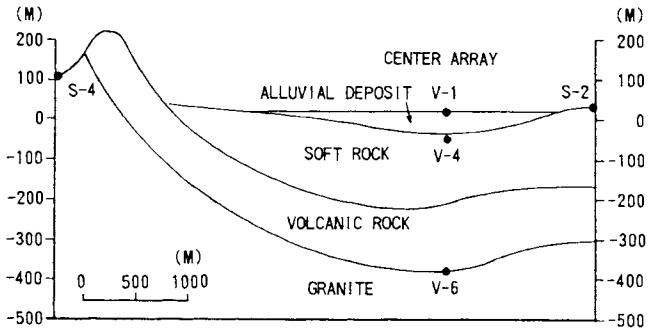

Figure 2 The cross section around the Center Array

Figure 2 illustrates the cross section along the line from S-4 point to S-2 point containing C.A.. This geological section was constructed from the results of bore hole investigation (B-1 and B-2), electric prospecting and in-site exploration. Table 1 shows the velocity structure of V-1～6 point which forms a vertical array. The data obtained from the P and S-wave velocities logging in the bore hole B-1 (the depth of 330m) and B-2 (the depth of 400m) are used in Table 1. The Q_s values are estimated using the formula proposed by Toki [2] in the case of V_s<400m/s. In the case of V_s >400m/s, these values are obtained from the mean values described in reference (3) on the Q_s values (; that is presented by the equation; $Q_s = V_s/32$). On the other hand, Q_p values are assumed as five times of Q_s values.

S-4 point on the ground would be considered to be the outcrop of a granite layer (V_s 2400m/s) in which V-6 point is set up. Likewise, S-2 point would correspond to the outcrop of a soft rock layer (V_s = 700m/s) in which V-4 point is set up. To examine amplification spectra, these outcrop points; S-2 and S-4 are chosen with V-1, V-4 and V-6 point forming a vertical array.

The estimation of responses due to P- and SV-wave are generally affected by the incident angle. Therefore, observed earthquakes to be examined in this study are limited to the ones of which apparent incident angles θ, defined by the epicentral distance Δ and the focal depth H at C.A. ($\theta = \tan^{-1}\Delta/H$), are as similar as possible. The epicenters of these earthquakes are shown in Figure 1 and the data of the earthquakes are indicated in Table 2. The mean value of apparent incident angle can be estimated at about 70° at C.A.. Figure 3 shows the examples of

Table 2 Data of analyzed earthquakes

NO	Date	Latitude	Longitude	Depth (km)	Δ (km)	θ (deg)	M
①	1985.05.11	37° 06.1′	141° 35.6′	45	127	71	5.3
②	1987.02.06[1]	36° 56.2′	141° 56.1′	30	160	79	6.4
③	02.06[2]	36° 57.7′	141° 53.8′	35	156	77	6.7
④	04.07	37° 18.0′	141° 52.0′	44	118	70	6.6
⑤	04.23	37° 05.3′	141° 37.6′	47	124	69	6.5

Table 1 Ground structures at the C.A.

INSTRUMENT DEPTH (m)	LAYER THICKNESS (m)	ρ (t/m³)	V_s (m/s)	V_p (m/s)	Q_s	Q_p
○ V-1 (-2m)	7	1.65	130	1300	10	50
	8	1.46	190	1300	10	50
	5	1.46	190	1300	10	50
	15	1.53	210	1300	10	50
	6	1.81	300	1300	10	50
	16	2.00	700	2000	22	110
○ V-4 (-57m)	23	2.00	700	2000	22	110
	75	2.07	1100	2500	33	165
	65	2.07	1100	2500	33	165
	35	2.24	1600	3200	50	250
	40	2.54	2700	4900	83	415
	30	2.24	1700	3200	56	280
	35	2.26	1600	3200	50	250
	40	2.23	2000	3500	63	315
○ V-6 (-401m)	——	2.34	2400	4500	—	—

both horizontal and vertical motions. The wave forms contain two main envelope shapes: Primary and Secondary portions. P-portion is defined by the duration starting from a P-wave arrival to a S-wave arrival. Secondary portion (S-portion) consisting of

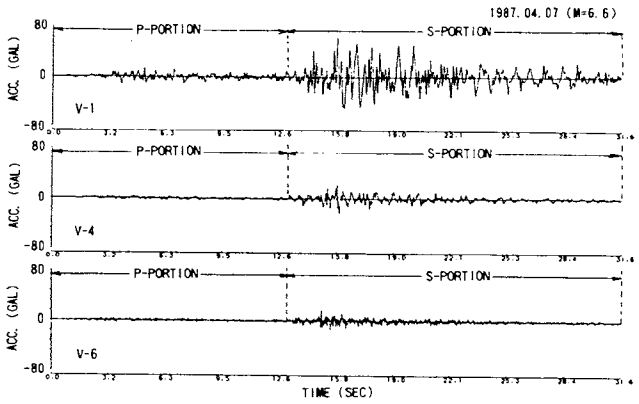

Figure 3(a) Examples of acceleration time history in vertical direction

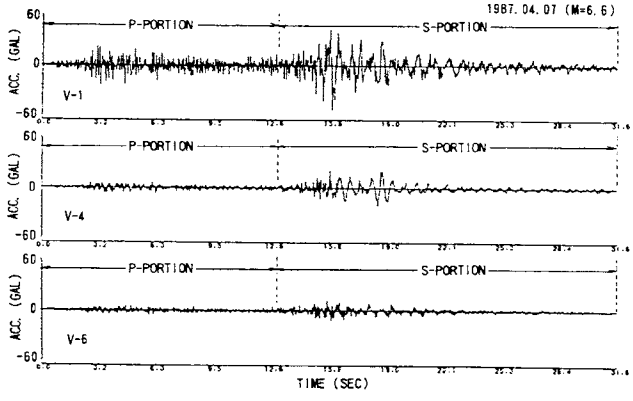

Figure 3(b) Examples of acceleration time history in horizontal direction

major envelope shape is assumed to have the duration time T_d, starting from arrival of S-wave, defined by Hisada and Ando [4] as written in the following equation.

$$T_d = 10^{0.31M - 0.774} \quad (1)$$

where M; magnitude
T_d ;duration time (sec)

In order to process the data based on P and SV-waves, horizontal waves in NS and EW directions are transformed into the epicentral and the transverse direction (L and T-direction), and in this study, the epicentral component (L-component) is assumed to represent horizontal motions induced by P and SV-wave. Wave trains in P and S-portion are assumed to be induced mainly P and SV-wave, respectively.

THEORETICAL AMPLIFICATION SPECTRUM

The theoretical amplification spectra are examined as a problem of P and SV-wave incidence to stratified structures. Silva's method [5] in which anelastic layers on an elastic half-space are considered is applied in the analysis. According to Silva, complex wave number vector $K_{P.S}$ is written as equation (2) with propagation vector $P_{P.S}$ and attenuation vector $A_{P.S}$. Then as shown in Figure 4, the angle between two vectors is equal to the incident angle and the direction of the vector $A_{P.S}$ is parallel to the z axis.

$$K_{P.S} = P_{P.S} - i A_{P.S} \quad (2)$$

and then $K_{P.S}$ is obtained from equation (3).

$$K_{P.S} = |K_{P.S}| = \frac{\omega^2}{V^2_{S.P}\left(1+\sqrt{1+Q^{-2}_{P.S}}\right)^2}\left(1-\frac{1}{Q^2_{P.S}}\right) \quad (3)$$

where $V_{P.S}$ presents the real part of complex velocity and $Q_{P.S}$ presents the Q value of P and S-waves.

The amplification spectrum to be calculated here implies not only the ratio between the motions at particular two points in the same structure, but also the ratio of an outcrop motion to the motion within the corresponding layer. The geological structure including the array observation system as shown in Figure 2 can be regarded as the stratified system. S-4 and S-2 points on the ground are assumed as respective outcrop of V-6 and V-4 point in the ground, and the ratios, V-1/V-4, V-4/V-6, S-4/V-6 and S-2/V-4 are calculated using the date in Table 2.

Following Silva's formulation, an extention of the Haskell-Thomson matrix method, the displacement potential matrix C_m at some mth layer can be presented as the following equation (4) with the matrix J and the stress-displacement matrix X_0 (Suffix 0 means "on the ground").

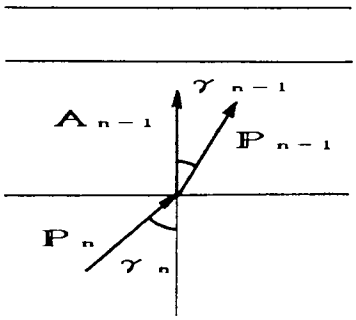

Figure 4 Specification of P,A and γ

$$C_m = J_m X_0 \quad (4)$$

where $C_m = [\ {}_mA_P + {}_mB_P,\ {}_mA_S + {}_mB_S,\ {}_mA_P - {}_mB_P,\ {}_mA_S - {}_mB_S\ ]^T$
$J_m = [\ {}_mJ_{ij}\ ]\ (i=j=4)$
$X_0 = [u_0, w_0, 0, 0]^T$
${}_mA_{P.S}$ and ${}_mB_{P.S}$;displacement potential amplitude
u_0;horizontal displacement on the ground
w_0;vertical displacement on the ground

Replacing m layers with n layers(;The n th layer is an elastic half space.), the surface displacement u_0 and w_0 is presented as equation (5) with the incident potential ${}_nA_P$ in the case of P-wave incidence to the n th layer.

$$\begin{aligned} u_0 &= -2[\ J_{22} + J_{42}\ ]\ {}_nA_P / R \\ w_0 &= 2[\ J_{21} + J_{41}\ ]\ {}_nA_P / R \\ R &= [\ J_{21} + J_{41}\ ][\ J_{12} + J_{32}\ ] - [\ J_{22} + J_{42}\ ][\ J_{11} + J_{31}\ ] \end{aligned} \quad (5)$$

In the same way, we can write the solution to the case of SV-wave incidence as equation (6) with the incident potential ${}_nA_S$.

$$\begin{aligned} u_0 &= 2[\ J_{12} + J_{32}\ ]\ {}_nA_S / R \\ W_0 &= -2[\ J_{11} + J_{31}\ ]\ {}_nA_S / R \end{aligned} \quad (6)$$

From the differential of the displacement potential, the displacement u_m and w_m of m th layer can be given as the function of the potential amplitude ${}_mA_{P.S}$ and the wave number $K_{P.S}$. Using equation (4), (5) and (6), u_m and w_m are expressed as the form of the product of incident potential amplitude ${}_nA_{P.S}$ multiplied by the formula composed of coefficients of wave number vector $K_{P.S}$ and matrix $J_{m.n}$.

Therefore, the amplification spectral ratios of m layer to another layer,in which ${}_nA_{P.S}$ can be neglected,are expressed by the formula composed of coefficients of $J_{m.n}$ and $K_{P.S}$. Since the outcrop displacement of m th layer is obtained from equation (5) or (6) adopted for n-m+1 layers' system, the amplification spectral ratio to the outcrop can be also calculated in the same manner.

Figures 5 and 6 show the amplification spectral ratios due to P-wave incidence in

vertical and horizontal directions respectively. In the same way, Figure 7 and 8 show the ratios due to SV-wave incidence.

In comparison between both spectral shapes in the case of P and SV-wave incidence, the shapes would be seen to be similar in the same direction in spite of different kind of waves (P and SV-wave); It is found that the shapes of the vertical ratios as shown in Figure 5 is similar to the same in Figure 7 as well as the shapes of the horizontal ratios in Figure 6 to that in Figure 8. In the range of incident angle in the calculations, the response of horizontal component due to P-wave and that of vertical component due to SV-wave give the minor amplitude respectively, and it is seen that the spectral ratios in the direction of the minor amplitude are inclined to indicate the great variation with frequency as shown in Figure 6 and 7. On the other hand, in the direction of the major amplitude, the shapes in the case of P-wave incidence as shown in Figure 5 are found to be identical and independent of incident angles. Moreover, the shapes in the case of SV-wave incidence as shown in Figure 8 are seen to be independent of the incident angles, although a little difference can be found in the case of the angle 30 ° . The amplification spectral ratio estimated by P and SV-wave incidence to the multi-layers system would be in dependent of the incident angles.

EXAMINATION ON OBSERVED AMPLIFICATION SPECTRA

It is assumed in this study that amplification spectra of observed motions can be obtained from the spectral ratios between particular two observation points. To estimate the observed spectral ratio, velocity response spectra (h=0%,where h shows the damping constant) are used because they are equivalent to Fourier amplitude spectra of acceleration motions. Thus, these spectral ratios between particular two points can be compared with the theoretical amplification spectral ratios described in the previous section.

Figures 9 and 10 show the spectral ratios on both the P-and S-portion of the vertical motions ((a) V-1/V-6 (b) V-1/V-4 (c) V-4/V-6 (d) S-2/V-4 (e)S-4/V-6). Comparing between the P- and S-portions, we can find that the shape of spectral ratio in the P-portion is similar for every earthquake, but less similar in the S-portion.

As shown in Figure 9 (b) and (c), spectral ratios in the low frequency range are inclined to be amplified in the rock layers ; the obvious resonant amplitude on V-4/V-6 exists at about 2.0Hz, while in the soil layers these resonant amplitude is inclined to exist in the high frequency range between 5Hz and 7Hz, and resonant amplitude on V-1/V-6 just exists at these frequencies. Concerning the outcrop and underground motions, the spectral shape of ratio S-2/V-4 is recognized to be similar to that of ratio V-1/V-4. On the other hand, the similarity of S-4/V-6 to V-1/V-6 is not so apparent as that of S-2/V-4 to V-1/V-4,

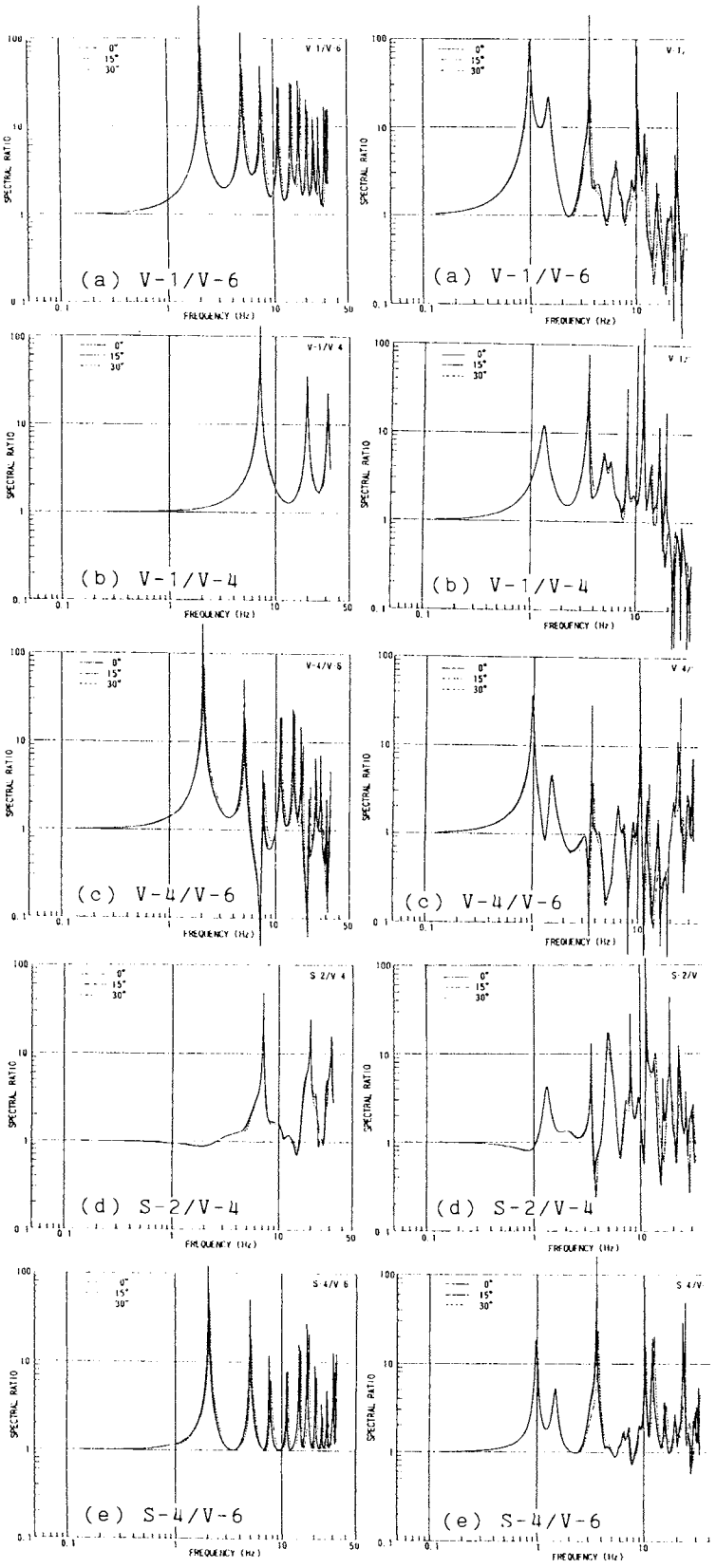

Figure 5 The spectral ratios due to P-wave incidence in vertical direction

Figure 6 The spectra ratios due to P-wave incidence in horizont direction

hough common resonant frequencies are ound. For the S-portion, in Figures 10 (a) ~ (e), there seems to be the same tendency s the P-portion. However, common resonant requencies are appeared to be not so emarkable as the P-portion.

We can compare these observed spectral atios on vertical motions with the heoretical amplification spectra described n the previous section. Here, an xamination was made on how spectral ratios n the P- and S-portions correspond to mplification spectra for the case of P- and -wave incidence respectively. Comparing he spectral ratios in the P-portion as hown in Figures 9 (a)~(e) with the heoretical ratios due to P-wave incidence, t can be found that the major resonant eak frequencies in the observed and heoretical ratios agree substantially. lthough the observed amplification factors re inclined to be smaller than the theoretical ones, it is recognized that the amplification spectra in the P-portion can e generally explained as a problem of P-ave incidence to multi-horizontal layers ystem. The same comparison on the pectral ratios in the S-portion as shown in Figures 10 (a)~(e) can not lead to the bvious conclusion as in the P-portion. That would be not only due to variable shapes of spectral ratios for every earthquake, but also due to the existence of different resonant frequencies from that of SV-wave incidence to multi-horizontal layers system. The example is indicated in the comparison of spectral ratio V-1/V-6 with the theoretical transfer ratio (compare Figure 7 (a) with Figure 10 (a))

An examination for the horizontal motions is shown next. Figures 11 and 12 illustrate spectral ratios on the P- and S-portion of the horizontal motions (; (a) V-1/V-6 (b) V-1/V-4 (c) V-4/V-6 (d) S-2/V-4 (e) S-4/V-6). In these figure ,we can find that the shapes of spectral ratios on the P-and S-portion are substantially similar. As described in previous section, both theoretical spectra of P-and SV-wave in horizontal direction are inclined to agree at first and second resonant frequency, and to disagree at higher resonant frequencies. Especially, amplification factors due to P-wave incidence are seen to be variable in the high frequency range. Therefore, the shapes of the observed spectral ratios on the P-and S-portion seem to be more fitted with those of theoretical spectral ratios due to SV-wave incidence than due to P-wave incidence. However,it is recognized that observed resonant frequencies are inclined to disagree with the theoretical ones as they become higher.

DISCUSSION

Because the theoretical amplification is independent of the incident angles (as far as the range is between 0° and 30°), the vertical component ratios on P-wave and the horizontal component ratios on SV-wave are shown to be expressed by the case that the incident angle on respective wave is 0 ° . Considering with the observed amplification ratio, the major resonant

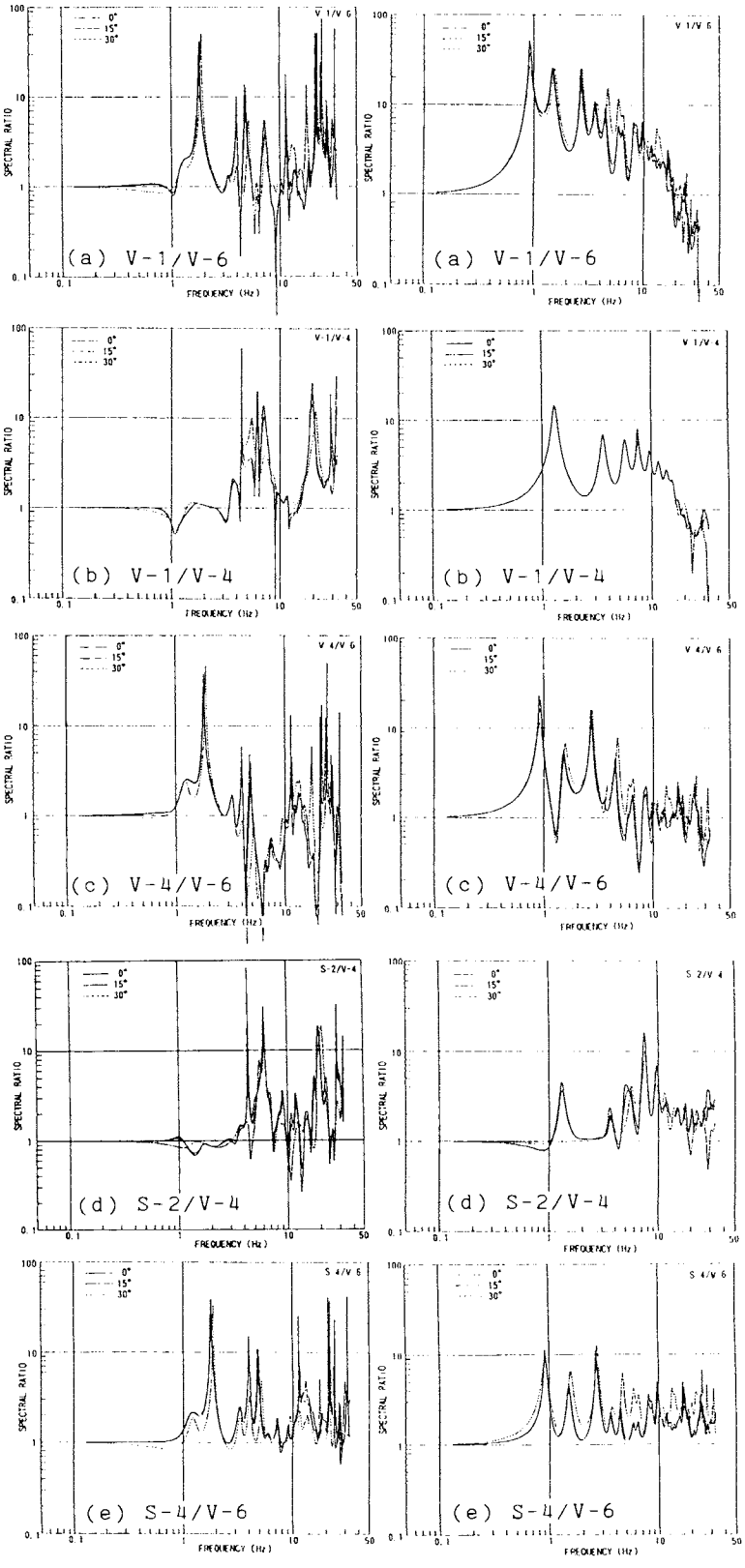

Figure 7 The spectral ratios due to SV-wave incidence in vertical direction

Figure 8 The spectral ratios due to SV-wave incidence in horizontal direction

frequencies which are the first,or sometimes the second, substantially coincide with the relating theoretical ones except for the case of the S-portion of vertical motions. That is, in vertical direction, the theoretical ratio due to SV-wave incidence can not explain the observed ratio of the S-portion appreciably. For this reason, it can be considered that the shapes of the observed ratios are not so similar for every earthquake,and that the theoretical ratios are greatly variable with the frequency due to the assumption of $Q_P = 5Q_S$. In addition, judging from the fact that the observed ratios are amplified in low frequency range, the existence of Rayleigh wave and the influence from the three-dimentional ground structure would be suggested. Especially, these ratios in the frequency range of lower than 1.0 Hz are inclined to be amplified as the motions propagate near the ground surface. This shows the influence due to the ground structure considering further depth and the surface wave resulting from this structure should be examined.

With regard to the S-portion in the horizontal motions,the observed amplification ratio due to No.1 earthquake(M=5.5),of which magnitude is the minimum value among the objective earthquakes, indicated more or less large values than that due to all other earthquakes. This fact would suggest that the Q_s value is dependent on the the magnitude of earthquake motions in this site and that the Q_s value decreases as the magnitude of earthquake motion increases.

The result from the comparison between the outcrop and underground motions shows that the shapes of the observed ratios on both S-2/V-4 and S-4/V-6 are similar to that of the theoretical amplification ratios respectively ,and from this fact, it is seen that both S-2 and S-4 motions could be regarded as the outcrop-motions of the same layer. We can also find that the topographic site effect would little exist at these outcrop points. However,as far as the S-portion in the horizontal motions is concerned, the amplification factors in the frequency range of higher than 10 Hz indicate six as the mean value(; about two or three times for the relating theoretical factor). It would be considered that this matter is caused by the influence from the surface weathering of the outcrop points judging from in-site conditions.

CONCLUSION

For the earthquake motions of which apparent incident angle is almost identical at C.A.site,horizontal and vertical acceleration time histories which have primary and secondary arrivals are selected and divided into P and S portions. Using these divided time histories,the ratios of response spectra between particular two points are calculated. In order to examine these ratios in the P- and S-portions,they are compared with the theoretical amplification spectra due to P- and SV- wave incidence to multi-horizontal layers system,and the following conclusions are

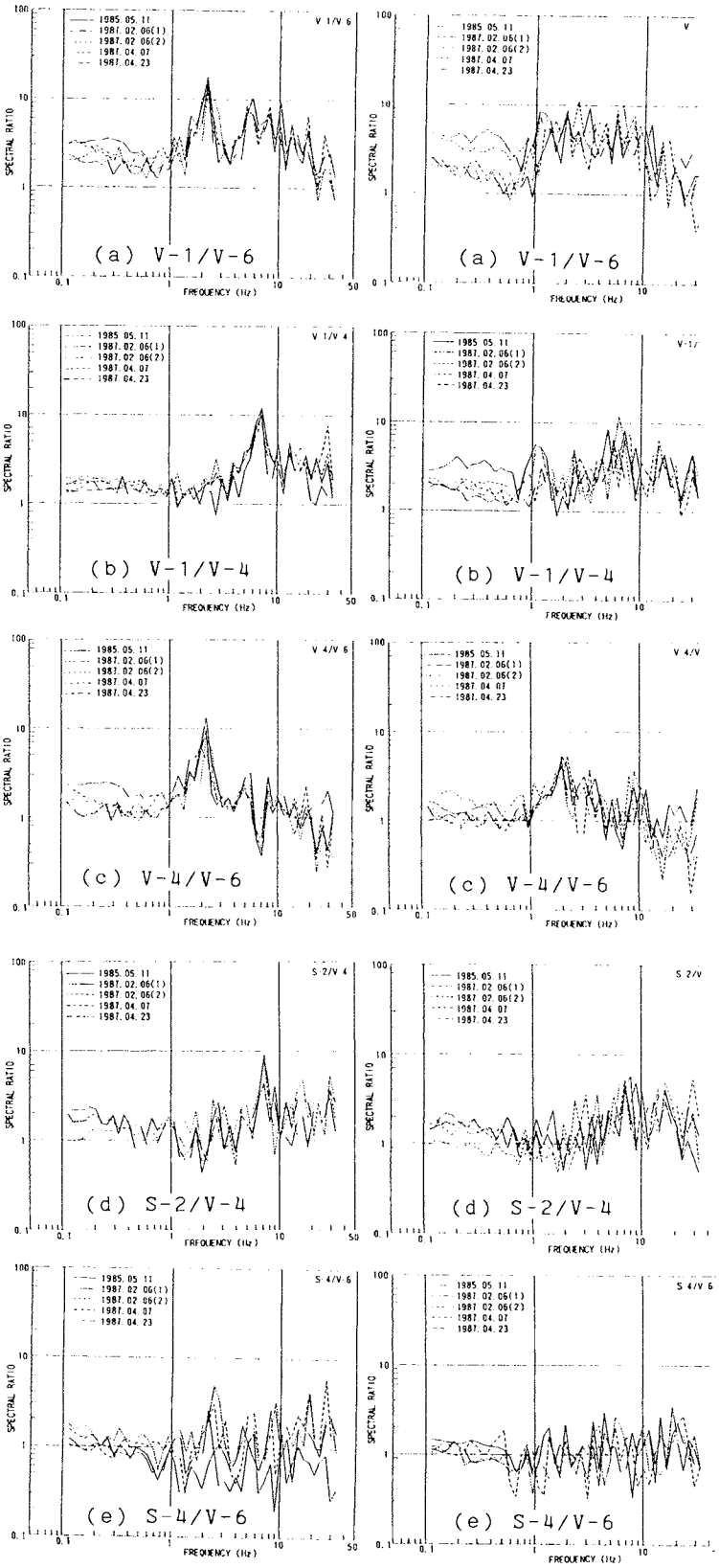

Figure 9 The spectral ratios on P-potion of vertical direction

Figure 10 The spectral ratios on S-potion of vertical direction

btained.

(1) The shape of the theoretical mplification ratios at C.A.site is little ependent on the incident angle on the ondition that the angle is between 0 ° nd 30° .

(2) The major resonant frequencies in he same direction for respective P- and SV- ave are identical, although the mplification spectral ratios in the irection of the minor amplitude are much ariable with frequency.

(3) In the vertical motions, the amplification spectral ratios in the P- portion can be explained by P-wave incidence into vertical direction. On the other hand, these ratios in the S-portion can not be found to be the clear relation with SV-wave incidence.

(4) In the horizontal motions, both amplification spectral ratios in the P- and S-portions are recognized to show the appreciable correspondence to the spectra due to SV-wave incidence in vertical direction around the major resonant frequency.

(5) In comparison between the outcrop and underground-motions, the major resonant frequencies seem to coincide with the theoretical ones obtained from multi-layers system. However, in the frequency range of higher than 10Hz, the amplification factors on both outcrop points are recognized to be amplified about two or three times for those under the ground, and this matter suggests that more consideration should be provided to predict the motions under the ground in direct use of the outcrop motions.

ACKNOWLEDGEMENT

The authors wish to express their gratitude to professor. M.Kamiyama of Tohoku Institute of Technology for his valuable advice.

REFERENCES

(1) Simizu,T.,Abe,K.,Kasuda,K,and Yanagisawa,E.(1988),Proc.9th WCEE,Vol.8,pp.137-142.
(2) Toki,K.(1981),Aseismic analysis of structure,Gihodo shuppan,p.79.
(3) Architectural Institute of Japan(1987),Seismic loading - state of the art and future developments
(4) Hisada,T. and Ando,H.(1976),Relation between duration of earthquake motion and the magnitude,K.I.C.T.
(5) W,Silva.(1976),B.S.S.A.,Vol.66,No.5, pp.1539-1554.

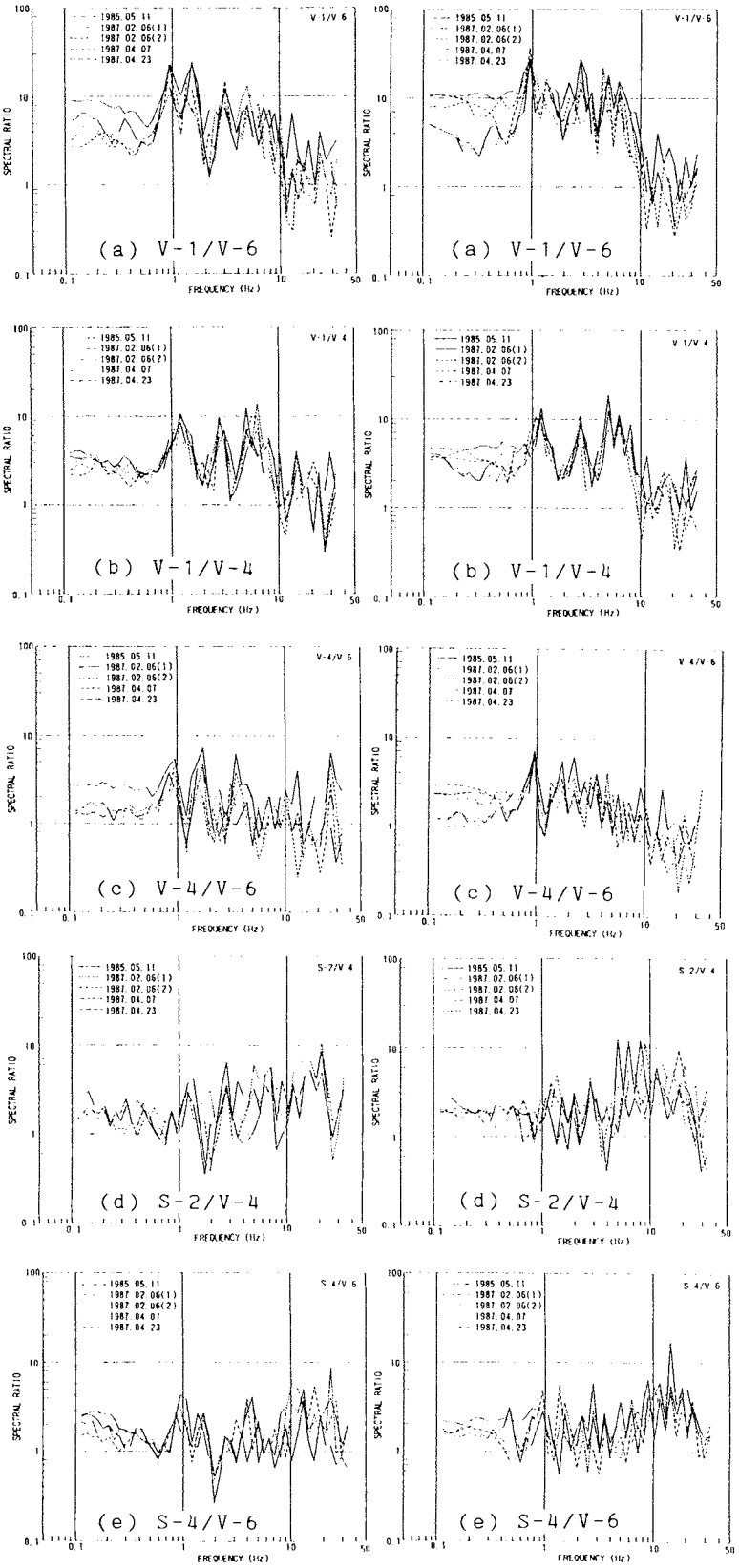

Figure 11 The spectral ratios on P-potion of horizontal direction

Figure 12 The spectral ratios on S-potion of horizontal direction